



## A source-to-structure method for the dynamic analysis of earth-rock dams

Q. Zeng<sup>(1)</sup>, X. Wang<sup>(2)</sup>, L. Zhang<sup>(3)</sup>, J. Wang<sup>(4)</sup>

<sup>(1)</sup> China Beijing, Department of hydraulic Engineering, Tsinghua University, zengqp19@mails.tsinghua.edu.cn

<sup>(2)</sup> China Beijing, Department of hydraulic Engineering, Tsinghua University,

<sup>(3)</sup> China Beijing, Department of hydraulic Engineering, Tsinghua University,

<sup>(4)</sup> China Beijing, Department of hydraulic Engineering, Tsinghua University, wangjt@tsinghua.edu.cn

### **Abstract**

Physics-based earthquake simulations are advancing to the research of seismic risk assessments as well as forward prediction in cases for which there are limited observations. This paper aims at simulating the 3D seismic wave propagation from the source to the high earth-rock dam with the local terrain. A two-step procedure is proposed using the spectral element method and the finite element method. Firstly, the ground motion at the dam-foundation interface is generated based upon the spectral element method, in which the source, the seismic propagation path and the local site features are considered. Secondly, the dynamic analysis of the earth-rock dam with a certain region of foundation is implemented by the finite element method with finer discretized meshes. In this way, the entire process of the seismic wave propagation and the fine analysis of the dam can be considered simultaneously. An earth-rock dam in southwest China is taken as an example to implement above-mentioned source-to-structure simulation. The effects of the high earth-rock dam and the source location of the scenario earthquakes on ground motions at the dam site are investigated. The simulated results demonstrate: (1) the dam body has an amplifying effect on the amplitude of seismic waves at the earth-rock dam site; (2) the seismic response of the dam generally gets stronger as the height of the earth-rock dam increases in the cross section; (3) the seismic response of the dam is larger in the middle part than those at the abutments in the transverse direction; (4) the effect of source, propagation path and local site on the seismic response of earth-rock dam should be taken into account.

*Keywords: Earth-rock dam; Ground motion; Spectral Element Method; Finite Element Method; Seismic response*



## 1. Introduction

The development of hydropower resources is concentrated in the area with rugged terrain, which is often accompanied by active tectonic movement. For this reason, the hydraulic infrastructure is often faced with seismic threat. The frequent occurrence of destructive earthquakes has caused a large number of engineering accidents, resulting in huge loss of life and property. Therefore, it is necessary to study the seismic characteristics on the local site and its dynamic response.

According to the relevant researches, it is found that the geological and topographical conditions on the dam site have a non-negligible influence to the actual seismic waves in this process. Zhang and Zhao<sup>[1]</sup> use the coupling method of finite and infinite element to find that the seismic amplification of Canyon topography is the most significant when the input angle of seismic wave is 90 degrees. He<sup>[2]</sup> also found that the canyon topography plays a significant amplification effect on the ground motion by analyzing the Newhall earthquake. However, few researches study the effect made by the dam itself. Considering the mass of the dam, the dam itself will cause significant changes in local terrain, so it is necessary to study the influence made by the dam itself.

When the seismic wave arrives at the site, this will cause dynamic response to the construction, which is the most important part of seismic safety evaluation. With the rapid improvement of computer, the Finite Element Method (FEM) has the strong ability to deal with complex conditions, widely used in various fields of engineering. Clough and Chopra<sup>[3]</sup> first used the FEM in two-dimensional plane strain analysis of earth rock dam. Angeliki and Jacob<sup>[4]</sup> conducted linear dynamic response analysis of earth-rock dams in the semi-circular canyon considering the dam body-foundation interaction. While as one of high-order finite element methods, the Spectral Element Method (SEM) with the advantage of high precision, rapid calculation can well simulate the ground motion propagation. Komatistch<sup>[5]</sup> used spectral element method to simulate the earthquake propagation process in Los Angeles basin. Magnoni<sup>[6]</sup> also used this method to simulate the L'Aquila earthquake. The above two methods can be well combined to analyze the whole process of seismic wave from generation to action. For this reason, this paper will simulate the 3D seismic wave propagation from the source to the high earth-rock dam with the local terrain, taking an earth-rock dam in southwest China as the example.

## 2. Seismic simulation

### 2.1 Preprocessing spectral element model

This 3D model, which measures approximately 20 kilometers long, 22 kilometers wide and 12 kilometers deep, is meshed by importing the terrain data from Google Earth. The grid size will affect the results: for one thing, if too large, it will not well reflect details of the structure; for another, if too small, it will generate a massive number of units, reducing computing efficiency significantly. Moreover, the impact of far field on ground motion to the site is limited. Therefore, as shown in Table 1, the transitional meshing method is used. The modified meshing program in the Specfem3d program is used to model. Then the total number of elements is about 5.21 million and the total degree of freedom is about 1.05 billion. The meshing grids under two conditions is shown in Figure 3, which can be seen that the combination of the dam with the terrain is coordinated and there is few deformed grids.

Table 1 –Transitional mesh structure

Number	Area	Mesh size	Remark
1	Far-field	180m×180m×180m	/
2	Dam-site	30m×30m×30m	area (8040m × 4760m × 3000m) around the site
3	Transition zone	60m×60m×60m	/

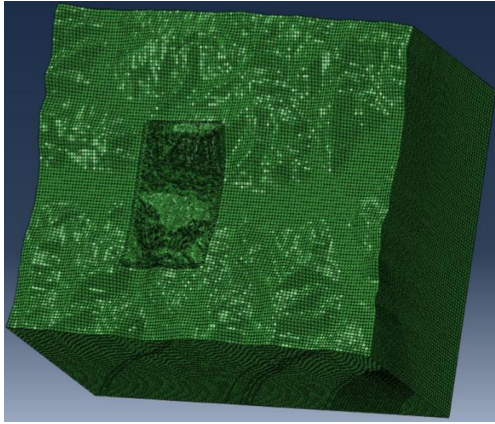


Fig. 1 – Spectral element model

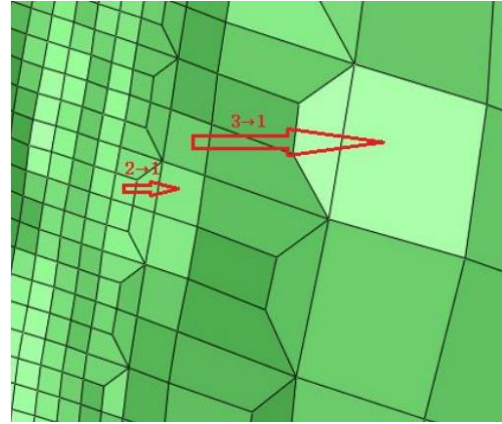


Fig. 2 – Transitional meshing

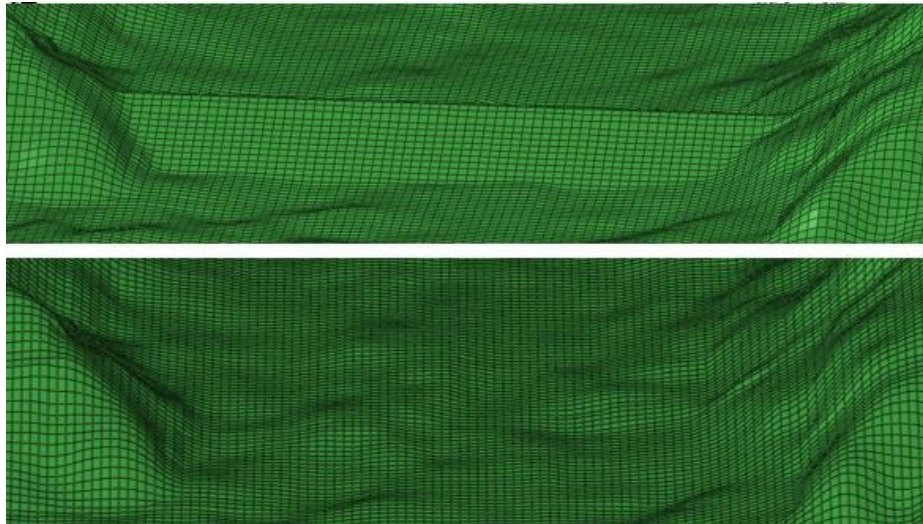


Fig. 3 – Meshing grids under two conditions (up: dam-existent; down: dam-nonexistent )

## 2.2 Source model and wave structure

The focal model is set as the point source, which is 1km below the center of the dam body; the magnitude of simulated earthquake is set as 4.0; the semiperiod of the source is set as 0.15s. Due to the increased probability of small-sized earthquakes near the dam site induced by the reservoir increases, these values are relatively reasonable for the study about the seismic response of the dam site. Seismic moment is obtained using the empirical equation<sup>[7]</sup> as follows: Eq. (1).

$$\log_{10} M = \frac{3}{2} M_w + 16.1 \quad (1)$$

in which  $M_w$  represents earthquake magnitude(Richter Scale),  $M$  is the seismic moment. Meanwhile, as shown in Fig. 3-5 schematic diagram of source fault, seismic moment tensor is usually represented by a symmetric matrix, which has six directional-components ( $M_{xx}$ ,  $M_{yy}$ ,  $M_{zz}$ ,  $M_{xy}$ ,  $M_{xz}$ ,  $M_{yz}$ ) obtained by the following equations: Eq.(2)~(7).

$$M_{xx} = -M(\sin\delta\cos\lambda\sin 2\phi + \sin 2\delta\sin\lambda\sin^2\phi) \quad (2)$$



$$M_{yy} = M(\sin\delta\cos\lambda\sin 2\phi - \sin 2\delta\sin\lambda\sin^2\phi) \quad (3)$$

$$M_{zz} = -(M_{xx} + M_{yy}) \quad (4)$$

$$M_{xy} = -M(\sin\delta\cos\lambda\sin 2\phi + \frac{1}{2}\sin 2\delta\sin\lambda\sin 2\phi) \quad (5)$$

$$M_{xz} = -M(\cos\delta\cos\lambda\cos\phi + \cos 2\delta\sin\lambda\sin\phi) \quad (6)$$

$$M_{yz} = -M(\cos\delta\cos\lambda\sin\phi - \cos 2\delta\sin\lambda\cos\phi) \quad (7)$$

in which  $\phi$  is strike-angle,  $\lambda$  is slip-angle and  $\delta$  is dip-angle. As for the point source, The strike angle of the fault is  $0^\circ$ , the dip angle  $90^\circ$ , the slip angle  $0^\circ$ . Then the moment tensor is represented by the Eq.(8).

$$M = \begin{bmatrix} M_{xx} & M_{xy} & M_{xz} \\ M_{xy} & M_{yy} & M_{yz} \\ M_{xz} & M_{yz} & M_{zz} \end{bmatrix} = \begin{bmatrix} 0 & 1.28 \times 10^{20} & 0 \\ 1.28 \times 10^{20} & 0 & 0 \\ 0 & 0 & 0 \end{bmatrix} \quad (8)$$

On account of the lack of measured geological data, the information out of the global crustal model of CRUST2.0 (Global crustal model at  $2^\circ \times 2^\circ$  degrees) or similar structural areas can be used to determine the seismic velocity structure of the site. The former method is used in this model with its parameters of the site are obtained as shown in table 2.

Table 2 –Parameters of wave structure

<b>P wave velocity</b> $V_p$ (m/s)	<b>S wave velocity</b> $V_s$ (m/s)	<b>Density</b> $\rho$ (kg/m <sup>3</sup> )
2500	1070	2110

### 2.3 Spectrum analysis

After preprocessing the model, those set values are input the into the open source code called specfem3d. Also, the number of calculation steps is up to 100000, setting the time-step as 0.0006s. Based on the principle of spectral element method (SEM), the propagation process in the initial 60 seconds is simulated under two conditions of the existence and non-existence of dam. Consequently, the simulated wave field results of time history and frequency spectrum is output, taking the measuring point in the center of dam axis and on the dam surface as concerned targets. Through these analyses, the seismic input and relevant conclusions of dynamic response of dam are obtained.

As shown in Figure 4, the acceleration amplitude values of frequency spectrum in the east-westward, north-southward and vertical directions are significantly higher than those in the absence of the dam in the spectrum range of low frequency (lower than 3Hz approximately). The largest spectrum difference of east-westward amplitude distributes near 1Hz, while the average difference is about 10 times below 1Hz and 10 times below 3Hz; the largest spectrum difference of north-southward amplitude distributes near 1Hz, while the average difference is about 5 times below 1Hz and about 7 times below 3Hz; the largest spectrum difference of vertical amplitude distributes near 1Hz as well, while the average difference is about 20 times below 1Hz and about 10 times below 3Hz. It can be concluded that the dam body has an amplification effect on the ground motion in the site area. The amplification effect in the direction parallel to the dam axis is more obvious than that perpendicular to the dam axis. In addition, Spectrum difference of the ground motion intensity in all directions decreases with increasing frequency. As for the significant amplification effect when frequency comes to 1Hz, it may be related to the fundamental frequency of the earth-rock dam structure.

The relative high frequency part ( $\geq 3\text{Hz}$ ) of acceleration spectrum tends to be overlapped and disordered,



which may be due to the lack of high frequency components excited by the source, so this paper does not analyze the high frequency components. Instead, the acceleration spectrum trend of dam surface points is basically consistent with that of foundation points, especially for the east-westward and vertical direction. However, the acceleration spectrum of dam surface points in the low frequency range is smaller than that of the ground point. Hence, the attenuation of seismic waves has a directional effect, which still needs further research.

As shown in Figures 5 to 7, under the dam-existent conditions, kinematic quantity (acceleration, velocity and displacement) amplitude values of time history are higher than those without dam, but their trend that both the peaks appear in the initial stage of the propagation process (about 0-5s) and the peak value under latter condition is slightly behind the former. Generally, when no dam body exists, the amplitude rapidly decays to zero within 20s, and then there is almost no fluctuation near the value of 0. By contrast, the amplitude still fluctuates significantly after its attenuation. The reason for this phenomenon can be that the seismic wave quickly releases energy to the free surface when no dam body exists, while the surface boundary will hinder the wave propagation as a result of continuous wave reflection inside the dam body after it propagates to the surface.

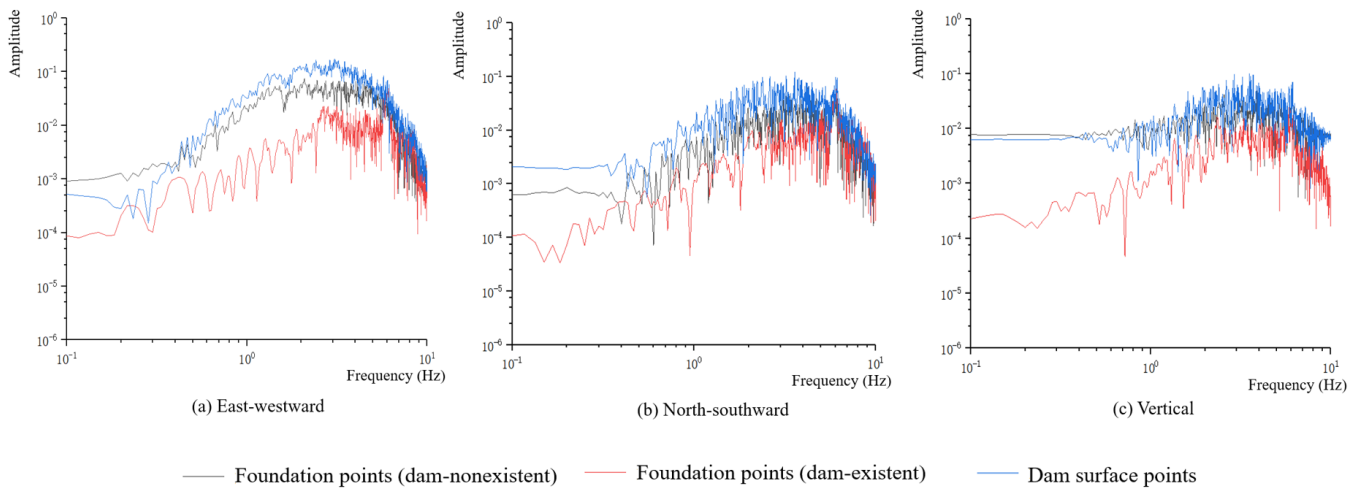


Fig. 4 – Acceleration spectrum

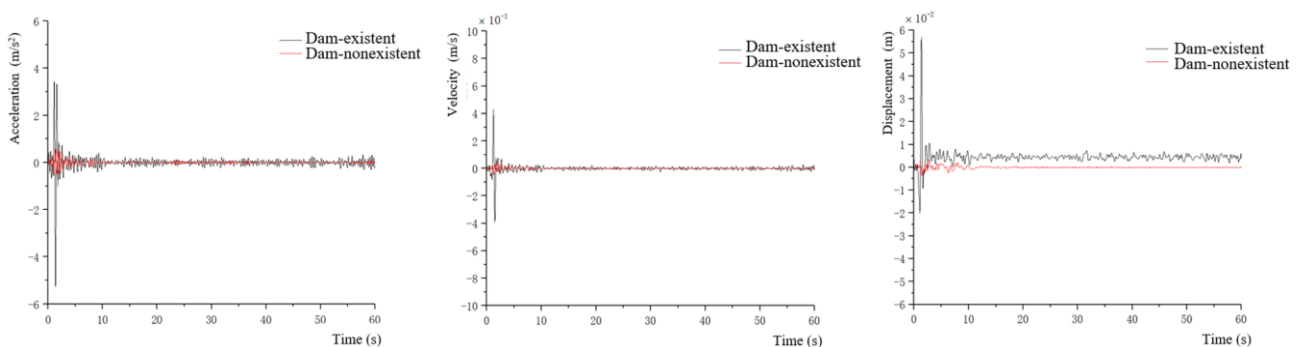


Fig. 5 – Time history in east-westward direction

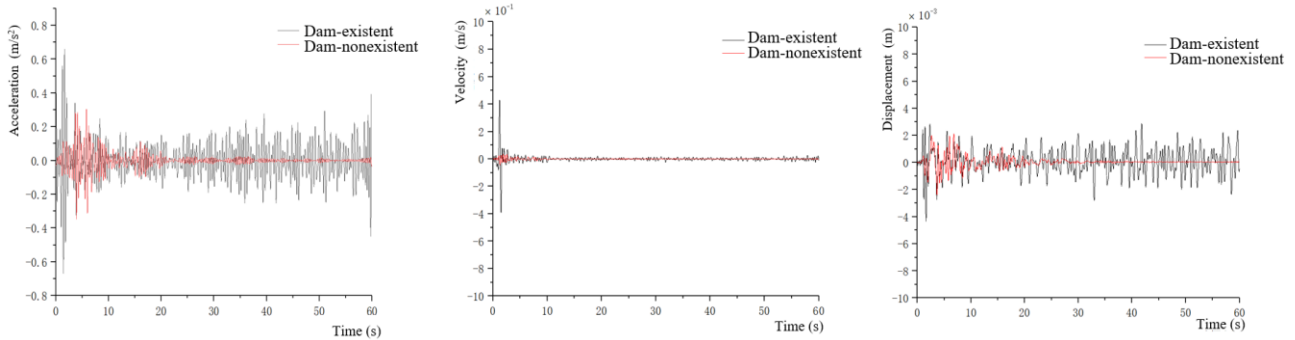


Fig. 6 – Time history in north-southward direction

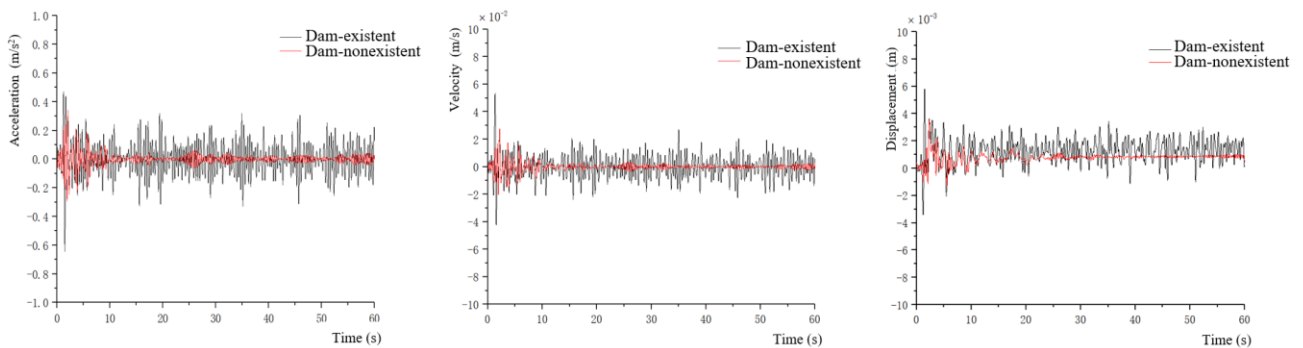


Fig. 7 – Time history in vertical direction

### 3. Dynamic response

#### 3.1 Calculation conditions

The material of earth-rock dam is nonlinear elasticity when yielding occurs under loads, resulting in elastic and irrecoverable plastic deformation, so the constitutive property must be expressed in nonlinear form. Mohr Coulomb model, an ideal nonlinear elastic-plastic model with a fixed yield surface<sup>[8]</sup>, is taken for analysis in this paper. A large number of experiments and engineering practices have proved that Mohr Coulomb model (MC model for short) has good applicability in reflecting the constitutive property of soil materials.

Due to the lack of material test parameters, as shown in Table 3, this paper selects the material parameters of a similar earth-rock dam in the local area. The simulated seismic wave is uniformly input into the finite element analysis model of earth-rock dam, so that the internal force of the structure at each time in the specific direction can be calculated, and the response (i.e. displacement, velocity and acceleration) at different times of the model can also be obtained. The calculation step of ground motion is 0.6s, and the duration is 60s with totally 1000 steps.

Table 3 –Parameters of materials

Area	Density $\rho/(kN/m^3)$	Elastic modulus $E/(GPa)$	Poisson's ratio $\nu$	Cohesion $c/(kpa)$	Internal friction angle $\varphi/^\circ$
Core wall	2087	5	0.35	30	27.9



Upstream transition zone	2100	15	0.3	0	31.7
Downstream transition zone	2100	15	0.25	0	30.8
Upstream rockfill zone	2284	75	0.2	0	35
Downstream rockfill zone	2284	75	0.2	0	35
Pre-loading zone	2200	50	0.21	0	35
Dam foundation	2300	73.8	0.2	5	38

### 3.2 Map of stress at different time

Through the acceleration curve of time history, it can be seen that the curve reaches to the peak at about 1.32s. Therefore, the results of different time ( $t_1=1.32s$ ,  $t_2=20.4s$ ,  $t_3=59.94s$ ) are compared. At 1.32s, the maximum principal stress boundary of tension and compression is located in the upstream rockfill area; the minimum principal stress boundary of tension and compression is in the middle of the downstream rockfill. The peak values of maximum principal stress are about 0.5MPa at the bedrock below the upstream rockfill, about 4MPa at the junction of the downstream rockfill and the ballast, and about 0.4MPa at the core wall. The overall level of Mises stress is the highest, about 4MPa, at the foundation under the core wall. Also, there is obvious stress concentration at the material interface between the upstream rockfill and the ballast, and the Mises stress in the middle of the core wall and the dam crest is minimum, only 0.05MPa. The characteristics of stress distribution at 20.4s and 59.94s are the same as that at 1.32s.

Hence, the region of tensile stress will expand from downstream to upstream as the increase of input seismic acceleration. In this process, the main stress in the upstream area is mainly compressive stress, while in the downstream area is mainly tensile stress, especially in the upper part of the core wall but the level of tensile stress is not high, which is within the strength range of dam material and with low risk of failure. The phenomenon of tensile stress concentration always exists at the junction of the downstream rockfill and the ballast. In practice, attention should be paid to the measures of seismic fortification in this area.

Table 4 –Peak values of stress

Time	Horizontal stress (Mpa)	Vertical stress (Mpa)	Minimum principal stress (Mpa)	Maximum principal stress (Mpa)	MISES stress (Mpa)
$t_1=1.32s$	-3.87	-4.40	-0.95	-6.09	0.05
	4.75	1.54	5.26	0.42	5.16
$t_2=20.4s$	-0.66	-1.34	-0.38	-1.13	0.002
	0.73	0.39	0.81	0.08	1.19
$t_3=59.94s$	-0.98	-1.12	-0.42	-1.18	0.003
	1.13	0.04	1.15	0.12	1.15

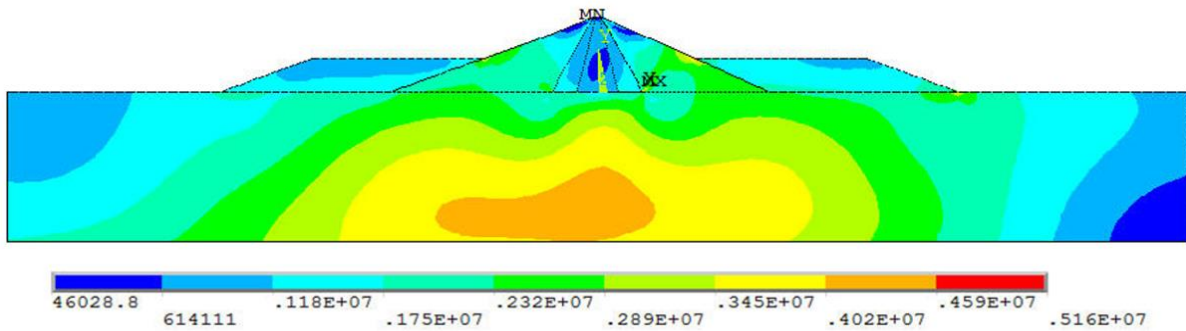


Fig. 8 – Map of MISES stress at 1.32s

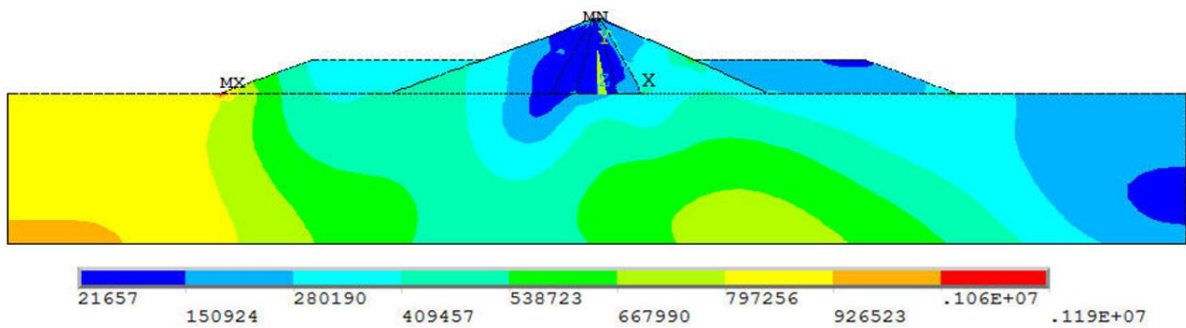


Fig. 9 – Map of MISES stress at 20.04s

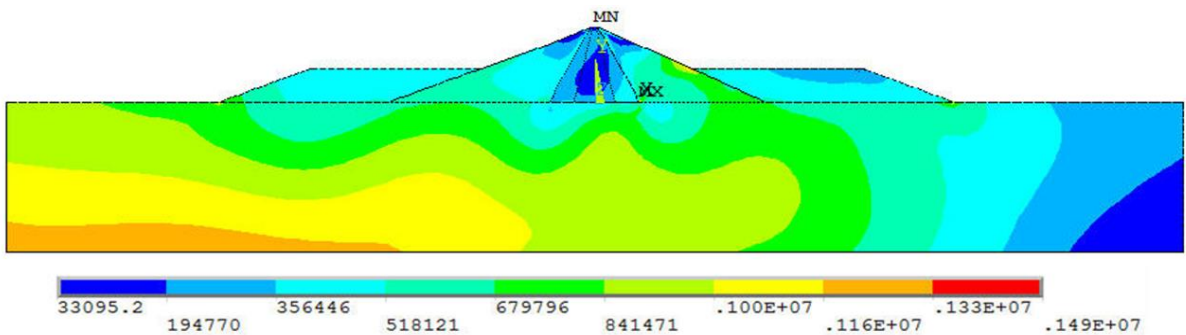


Fig. 10 – Map of MISES stress at 59.94s

### 3.3 Seismic response of different sites

In order to study the response characteristics of different sites on the dam body, as shown in Figure 11, five sites on the dam are selected for analysis. Among them, #2 is the top site of upstream ballast; #972 is the site on the packway of the upstream rockfill area; #992 is the site on the crest; #2396 is the site on the packway of the downstream rockfill area; #3293 is the top site of downstream ballast.

Under the joint action of horizontal and vertical earthquakes, the horizontal displacement of the dam body at node 2 is 4.79cm in the upstream ballast, and 8.32cm in the upstream rockfill area; the maximum horizontal displacement of the top node of the dam is 8.28cm, and the maximum horizontal displacement of the node at the downstream rockfill area is 8.42cm. By the charts, the time history of each motion component





is basically consistent with the waveform of seismic wave. With the increase of dam height, the response of displacement, velocity and acceleration of the dam body increases.

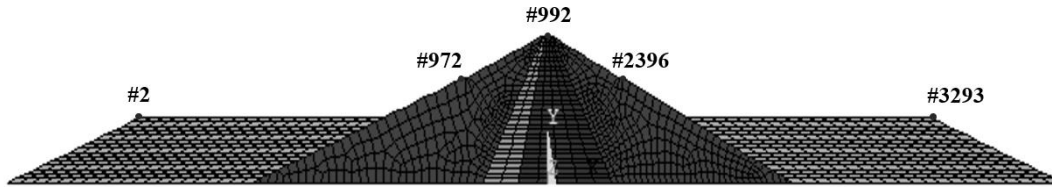


Fig. 11 – Selected sites on the dam

Table 5 –Peak values of nodes

Node number	Maximum displacement in X direction (cm)	Maximum displacement in Y direction (cm)	Maximum velocity in X direction (m/s)	Maximum velocity in Y direction (m/s)	Maximum acceleration in X direction (m/s <sup>2</sup> )	Maximum acceleration in Y direction (m/s <sup>2</sup> )
#2	4.79	0.68	0.60	0.078	8.29	1.01
#972	8.32	0.38	1.06	0.037	14.77	0.42
#992	8.28	0.40	1.05	0.046	14.62	0.64
#2396	8.42	0.57	1.07	0.083	14.92	0.96
#3293	4.94	0.14	0.62	0.022	8.46	0.33

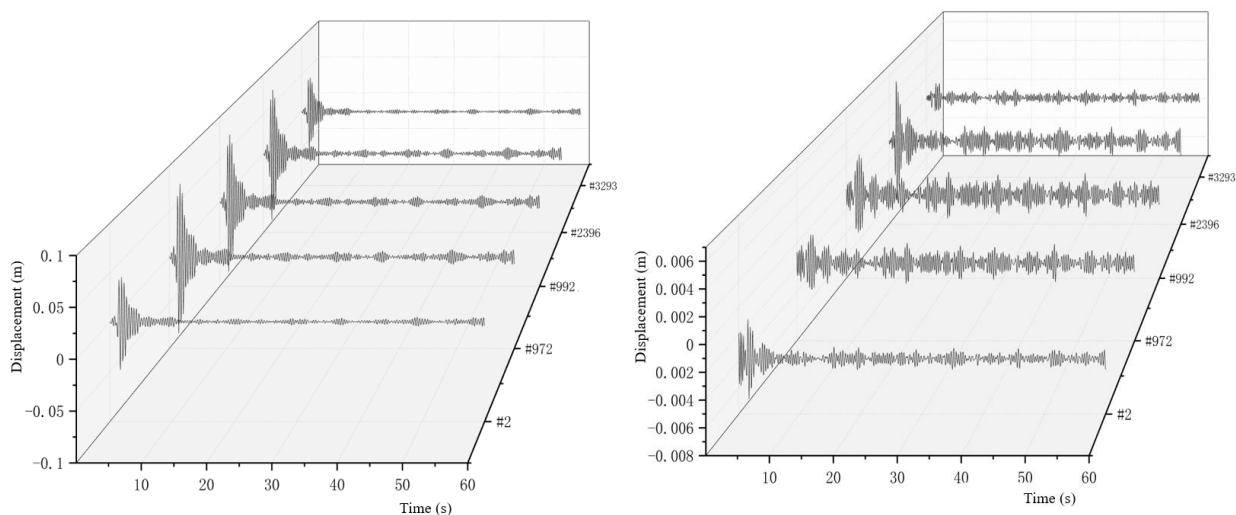


Fig. 12 – Time history of displacement on different sites (left :X direction; right: Y direction )

### 3.4 Spatial stress distribution

At the moment of 1.32s, the maximum MISES stress of one side section (y=800m) is 12Mpa on the dam crest, and tensile stress of the core wall reaches to about 0.8MPa. While in the middle



section(y=1400m), the maximum MISES stress is much higher. The tensile stress at the top of the core wall is about 1MPa. the maximum MISES stress of another side section(y=2000m) is 12Mpa on the dam crest, too, and tensile stress of the core wall reaches to about 1.8MPa. Also, there exists a large region of tensile stress on the upper and lower bedrock surface. The characteristics of spatial stress distribution at 20.4s and 59.94s are the same as that at 1.32s. As far as the qualitative law is concerned, tensile stress response are prone to exist in the upstream rockfill area and the upper part of the core wall. In the perpendicular direction to river course, the stress and the response near the dam abutment on both sides is less obvious than that of the middle part.

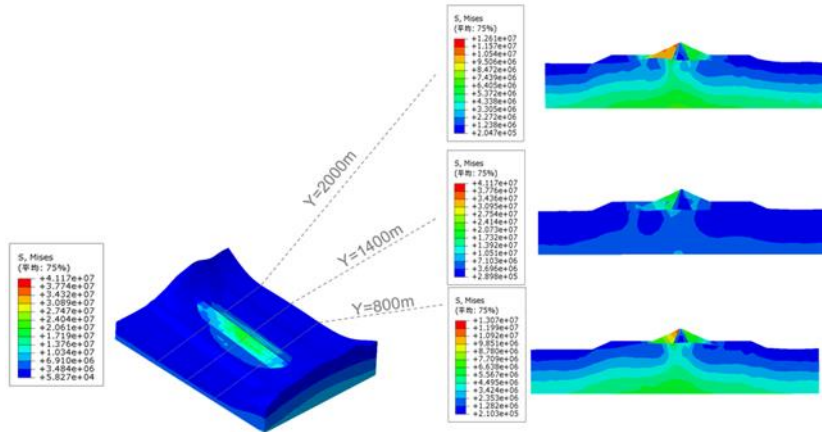


Fig. 13 – Map of spatial stress at 1.32s

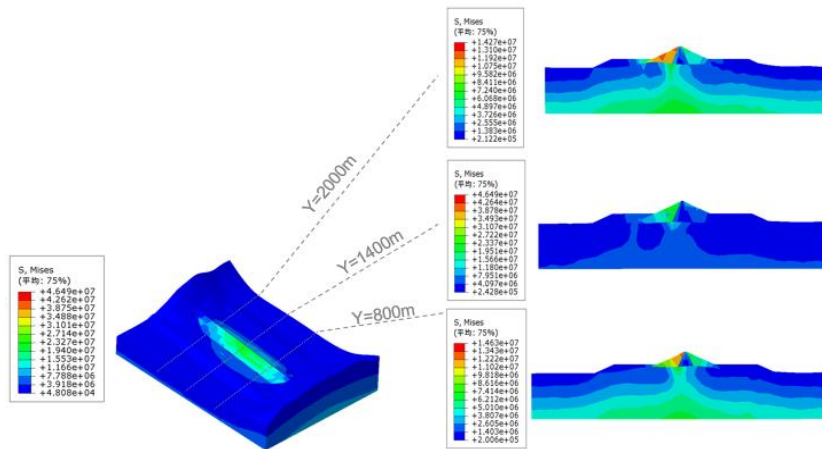


Fig. 14 – Map of spatial stress at 20.04s

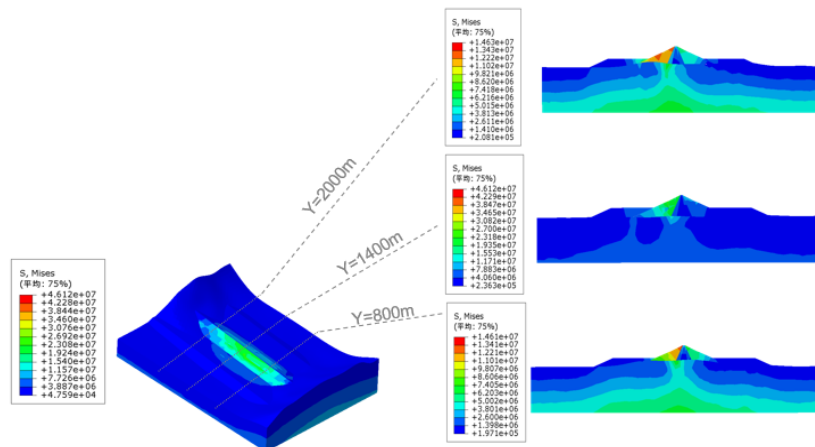


Fig. 15 – Map of spatial stress at 59.94s

#### 4. Conclusion

In this paper, An earth-rock dam in southwest China is taken as an example to implement above-mentioned source-to-structure simulation. According to the existing engineering data, the seismic wave propagation from the source to the dam site is simulated based on the wave theory and the spectral element method. The two-dimensional typical section of earth rock dam and the three-dimensional finite element model with the local terrain are established.

The response results of earth rock dam under different conditions of completion period and normal period are considered respectively considering materials property and uniform input. Through comparison, these conclusions are obtained: (1)with regional homogeneous material model, for the earthquake excited by superficial source under the dam body, the dam itself will amplify the seismic in all directions; (2) Generally, strong arch effect appears at the bottom of dam, especially on the upper part of core wall (4/5 of the dam height) and the interface between transitional layers. Then, the arch effect is so as to impounding period but is a little weakened; (3) The time history trend of each motion component for characteristic points is basically the same as that of the seismic wave, and the variation of time history on the dam crest is determined by the seismic waveform and the constitutive characteristics of the earth-rock dam. With the increase of dam height, the amplification of motion component gets obvious. And at the position where the water stop is relatively weak, the dynamic tensile stress appears local stress concentration. Under the same input condition, the distribution phase of dam dynamic response value shows the characteristics of large in the middle and small on both sides.

#### 5. References

- [1] Chuhan, Z. , & Chongbin, Z. (1988): Effects of canyon topography and geological conditions on strong ground motion. *Earthquake Engineering and Structural Dynamics*, 16(1), 81-97.
- [2] He, Chun Hui , et al. "Simulation of broadband seismic ground motions at dam canyons by using a deterministic numerical approach." *Soil Dynamics and Earthquake Engineering* 76.Complete(2015):136-144.
- [3] Clough R W, Chopra A K. (1966): Earthquake stress analysis in earth dams. *Journal of the Engineering Mechanics Division*, ASCE, 92(2): 197-212.
- [4] Angeliki P, Bielak J(2001): Seismic elastic response of earth dams with canyon interaction[J]. *Journal of Geotechnical and Geoenvironmental Engineering*, 127(5): 446-453.



- [5] Komatitsch, & D. (2004): Simulations of ground motion in the los angeles basin based upon the spectral-element method. *Bulletin of the Seismological Society of America*, 94(1), 187-206.
- [6] Magnoni, F. , Casarotti, E. , Michelini, A. , Piersanti, A. , Komatitsch, D. , & Peter, D. , et al. (2014). Spectral-element simulations of seismic waves generated by the 2009 L'Aquila earthquake. *Agü Fall Meeting. AGU Fall Meeting Abstracts*.
- [7] Hanks T C , Kanamori H (1979),. Moment magnitude scale. *Journal of Geophysical Research Atmospheres*, 84(B5): 2348-2350.
- [8] Escartín, J., Hirth, G. , & Evans, B. . (1997): Nondilatant brittle deformation of serpentinites: implications for mohr-coulomb theory and the strength of faults. *Journal of Geophysical Research*, 102(B2), 2897.
- [9] Zhang C H (2013). *Seismic safety of concrete dams*. Oxford: Butterworth- Heinemann.
- [10] Wang, J. T. , Zhang, C. H. , & Jin, F. . (2012). Nonlinear earthquake analysis of high arch dam–water–foundation rock systems. *Earthquake Engineering & Structural Dynamics*, 41(7), 1157-1176.
- [11] Zhang, S. , & Wang, G. . (2013). Effects of near-fault and far-fault ground motions on nonlinear dynamic response and seismic damage of concrete gravity dams. *Soil Dynamics and Earthquake Engineering*, 53, 217-229.
- [12] Dakoulas, P. . (1993). Response of earth dams in semicylindrical canyons to oblique sh waves. *Journal of Engineering Mechanics*, 119(1), 74-90.